RSC Mechanochemistry

ROYAL SOCIETY OF CHEMISTRY

PAPER

View Article Online
View Journal | View Issue

Cite this: *RSC Mechanochem.*, 2024, **1**, 492

Efficient mechanochemistry of beta blockers: neutralization, salification, and effect of liquid additives†

Delbert S. Botes, [ab] Jesus Daniel Loya, [b] Mahboubeh Ghahremani, [b] Bailee B. Newham, [b] Mikaela I. Aleman, [b] Gary C. George, III, [ab] Daniel K. Unruh [b] and Kristin M. Hutchins *[abc]

Beta blockers are a class of ubiquitous cardiovascular drugs that have collectively received little attention from a crystal engineering standpoint. Here, we describe the use of mechanochemistry in the salification of five beta blockers (propranolol, metoprolol, acebutolol, atenolol, and labetalol) with nicotinic and isonicotinic acid. Firstly, liquid assisted grinding (LAG) was used to neutralize the commercial beta blocker salts, enabling the efficient gram-scale formation of the free bases, which are essential for cocrystallization. Thereafter, 1 : 1 mechanochemical cocrystallizations were successful in all but one case and nine salts were characterized, eight of which are novel. Furthermore, the racemic free base crystal structure of acebutolol is reported for the first time, as well as the first multicomponent crystal of labetalol that is not a simple salt. Salification was enabled by the large pK_a differences between the components, which facilitated the protonation of the basic amine on the beta blockers' alkanolamine skeleton. Thereafter, charge-assisted hydrogen bonding promoted cocrystallization. We envisage salification to be applicable to any beta blocker, considering the current study encompasses approximately one quarter of this drug class. Lastly, the role of different liquid additives in the LAG process was assessed, and the solvent identity was found to play a substantial role in the mechanochemical outcome, although it did not strictly correlate with polarity. This study demonstrates that LAG screening with a wide selection of solvents provides a path to achieve full conversion to products, explore the crystal landscape of multicomponent crystals, and assist in identifying additional phases and/or late stage polymorphs in solid form development.

Received 18th July 2024
Accepted 17th August 2024

DOI: 10.1039/d4mr00078a

rsc.li/RSCMechanochem

Introduction

Mechanochemistry has been demonstrated as a vital technique in the toolbox of crystal engineers.[1] Since the first reported mechanochemically facilitated and pharmaceutically relevant cocrystallizations involving adenine and thymine derivatives,[2] as well as sulfadimidine with several aromatic carboxylic acids,[3] the utilization of mechanochemistry for multicomponent crystal synthesis has risen in popularity.[4]

Multicomponent crystals, particularly cocrystals and salts,[5] are relevant in the pharmaceutical industry as they present opportunities for enhancing properties of active pharmaceutical ingredients (APIs).[6,7] Such multicomponent solids are formed *via* cocrystallization, the process of combining at least two compounds to generate a unique solid phase. Formation of intermolecular forces between the different compounds facilitates cocrystallization of the components. In cocrystals, the components interact through neutral interactions, such as hydrogen or halogen bonds, while in salts, ionic bonding exists between the components as a cation and anion are formed by the transfer of an ionizable proton from one component to another. Specifically, cocrystals and salts can possess advantageous physicochemical properties such as improved solubility,[8] stability,[9] tabletability,[10] permeability,[11] and overall bioavailability,[12] all without any modifications to the chemical structure of the API. This provides an attractive avenue toward improving the pharmacokinetics of new and existing APIs, especially considering that the majority of marketed and in-development drugs possess less than ideal characteristics and do not fall into the Biopharmaceutical Classification System (BCS)[13] Class I

[a]*Department of Chemistry, University of Missouri, 601 S. College Avenue, Columbia, MO 65211, USA. E-mail: kristin.hutchins@missouri.edu*

[b]*Department of Chemistry and Biochemistry, Texas Tech University, 1204 Boston Avenue, Lubbock, TX 79409, USA*

[c]*MU Materials Science & Engineering Institute, University of Missouri, Columbia, MO 65211, USA*

† Electronic supplementary information (ESI) available: Experimental details, pK_a calculations, single-crystal X-ray data and structural descriptions, PXRD data, NMR spectra, thermal data. CCDC 2371670–2371679. For ESI and crystallographic data in CIF or other electronic format see DOI: https://doi.org/10.1039/d4mr00078a

category (high solubility and high permeability).[14] Furthermore, more efficacious formulations can be discovered through the combination of APIs for enhanced therapeutic effects,[15] as in the U.S. Food and Drug Administration (FDA) approved cocrystals, Entresto®[16] and Seglentis®.[17] Cocrystallization also presents ample opportunities in intellectual property creation and extension.[18]

Identifying favorable intermolecular interactions between molecules aids in achieving cocrystallization. Viable coformers[19] are often selected from the FDA's Substances Added to Food list which, in particular, includes a subsection of Generally Recognized as Safe (GRAS) substances.[20] Examination of the functional groups on the pharmaceutical and the coformer, as well as what types of synthons they engage in, aids in the design and synthesis of cocrystals and salts. Additionally, the pK_a rule provides an empirical guide for whether a cocrystal or a salt will form.[21,22]

Traditionally, the most common way of preparing multicomponent crystals is *via* slow solvent evaporation. This process can be time consuming and relies heavily on the solubilities of the components in the chosen solvent(s).[23] Mechanochemistry presents a green alternative as either no solvent (neat) or minimal solvent (liquid assisted grinding, LAG) is employed with an outcome often obtained in a quicker timeframe.[24] Whether performed manually using a mortar and pestle or automatically using a mill or mixer, mechanochemistry has revealed unique crystal forms that cannot be obtained through conventional means.[1,4,25]

Our group has recently shown the applicability of mechanochemistry in facilitating the cocrystallization of liquid compounds,[26] as well as its utility in accomplishing the reversible interconversion of pharmaceutical salt polymorphs.[27] The amount of solvent used in LAG (defined by the η-parameter, the ratio of the volume of solvent (μL) to mass of reactants (mg))[28] as well as solvent identity can be crucial to the milling outcome.[29] A recent study of ritonavir, a drug whose manufacturing history exemplifies the importance of solid form development, has illustrated the tremendous benefits of LAG in controlling polymorphism.[30]

One of our interests lies in investigating cocrystallization opportunities with APIs that have not been extensively studied. Beta blockers, a class of APIs that act as antagonists of adrenergic receptors and are used to treat cardiovascular diseases,[31] are widely used, with more than 20 available commercially,[32] but have collectively received little attention from a crystal engineering standpoint. Compounds in this class are chiral, possessing one or more stereogenic centers and a skeleton comprised of an alkanolamine, which we envisaged could be utilized for cocrystallization. We chose to study five of these APIs, namely propranolol (**Pro**), metoprolol (**Met**), acebutolol (**Ace**), atenolol (**Ate**), and labetalol (**Lab**) (Fig. 1, left). **Pro**, **Met**, and **Lab** fall into BCS Class I (high solubility and permeability) while **Ace** and **Ate** are Class III (high solubility and low permeability) drugs.[33,34]

Pro is a first-generation beta blocker (non-selective β blocker) and was the first commercialized. **Met**, **Ace**, and **Ate**, are second generation beta blockers (selective β_1 blockers) while **Lab** is of the third generation (antagonist of both α and β receptors).[31,35] Beta blockers are available commercially as racemic mixtures (here **Pro**, **Met**, **Ace**, and **Ate** all have one stereocenter) or an equal mixture of stereoisomers (*ca.* 25% each of the four stereoisomers for **Lab** with two stereocenters). Furthermore, beta blockers are often sold as salts. **Pro**, **Ace**, and **Lab** are sold as hydrochloride salts, **Met** is available as a tartrate salt, while **Ate** is sold as the free base.

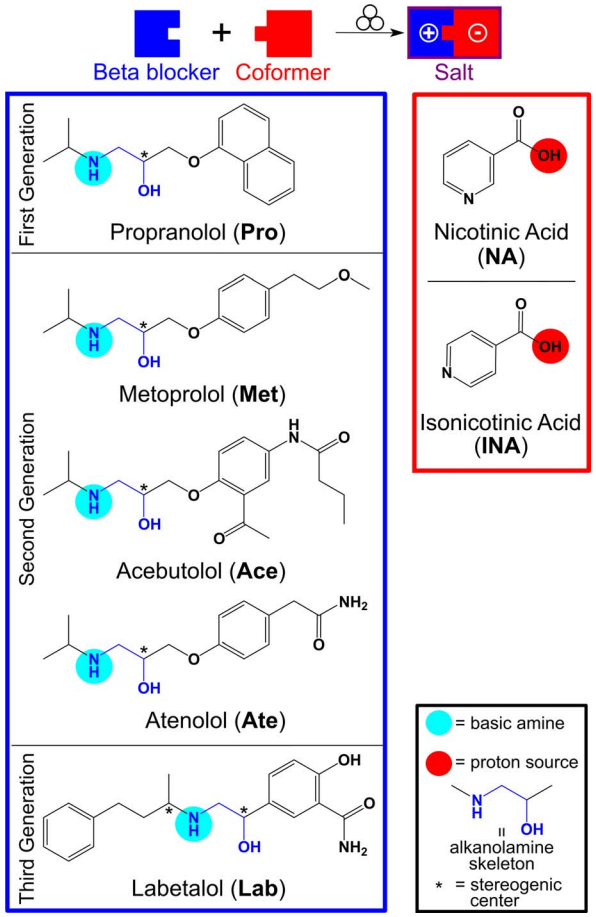

Fig. 1 Outline of the work investigated in this paper. Five beta blockers from the three different generations, namely, **Pro**, **Met**, **Ace**, **Ate**, and **Lab**, were studied mechanochemically to assess their suitability in forming salts with **NA** and **INA**. The basic nitrogen atoms were targeted *via* protonation from the acids.

A search of the Cambridge Structural Database (CSD) revealed that our five selected beta blockers have been successfully crystallized before. Specifically, the free base structures of **Pro**, **Met**, and **Ate** are known, and there are multicomponent solids reported with **Pro** (16), **Met** (10), **Ace** (2), and **Ate** (4). Notably, only one structure with **Lab** has been published, a hydrochloride salt.[36] All previously reported multicomponent solids are salts, following the pK_a rule,[21,22] and most of the reported salts are based on simple counterions (*e.g.*, Cl^-) or acids (*e.g.*, succinic, oxalic, fumaric, benzoic derivatives). Most structures involve racemic mixtures of the beta blocker, although a few cocrystallizations of a single stereoisomer or conglomerate have been reported (Table S1, ESI†). Across all the

salt structures of these beta blockers, proton transfer to the basic amine on the alkanolamine skeleton is a common characteristic. However, no systematic studies of multiple beta blockers together with applicable coformers have been reported; thus, we sought to synthesize salts of **Pro**, **Met**, **Ace**, **Ate**, and **Lab** together with nicotinic acid (**NA**) (niacin, a form of vitamin B_3 and a GRAS compound) or isonicotinic acid (**INA**), a structural isomer of **NA** (Fig. 1). **NA** has been used to reduce cholesterol and cardiovascular events, making it an interesting coformer for formulation with beta blockers.[37–39]

Here, we demonstrate the use of mechanochemical methods for both neutralization and salification of beta blockers. Mechanochemistry is first applied to the gram-scale neutralization of commercial salts to isolate the free base of each beta blocker, and subsequently, mechanochemistry is used in salification to prepare a series of pharmaceutical salts containing beta blockers. The impact of solvent additives in LAG is also assessed, and although correlation to solvent parameters is not trivial, solvents with higher polarity tend to afford salt formation, while low polarity solvents afford lower conversion. We also obtained the free base structure of the drug **Ace** for the first time and show the first cocrystallization of **Lab** not involving a simple counterion. This work demonstrates the significant influence of liquid additive identity in achieving conversion to multicomponent solids through LAG and highlights the power of LAG screening to assess solid forms of APIs.

Experimental

Materials

Met tartrate, **Ate**, and **NA** were purchased from Tokyo Chemical Industry Co., Ltd (Toshima, Kita, Tokyo, Japan). **Ace HCl** was purchased from Fisher Scientific (Lenexa, KS, USA) while **Pro HCl** and **INA** were purchased from Oakwood Chemical (Estill, SC, USA). Additional **Ate** and **Ace HCl** were purchased from Combi-Blocks (San Diego, CA, USA). **Lab HCl** was purchased from Sigma-Aldrich (St. Louis, MO, USA) and AA Blocks (San Diego, CA, USA). All solvents, namely, acetone, acetonitrile, chloroform, dichloromethane, diethyl ether, *N*,*N*-dimethylformamide, ethanol, ethyl acetate, hexanes, isopropanol, methanol, tetrahydrofuran, and toluene were purchased from Fisher Scientific (Lenexa, KS, USA). Reagents and solvents were used as received without further purification.

Mechanochemistry

Milling experiments were performed using a FlackTek SpeedMixer DAC 330-100 SE purchased from FlackTek Manufacturing. Experiments were conducted in either 5 or 15 mL stainless steel jars with either 7 mm or 10 mm ⌀ stainless steel grinding balls, both obtained from Form-Tech Scientific. A custom holder acquired from Form-Tech Scientific was used to hold the milling jars in the SpeedMixer. Experiments were performed at a frequency of 1500 rpm for various times. The SpeedMixer was operated for a maximum of 5 minutes with a 30 second rest period required thereafter. For experiments longer than 5 minutes, multiple rounds of milling were performed (*e.g.*, 6 minutes of milling were performed in two rounds of 3 minutes and 20 minute experiments performed as four 5 minute sessions).

Neutralization of commercial beta blocker salts

All studied beta blockers, with the exception of **Ate**, required the isolation of the free base form from the commercially purchased chloride (**Pro**, **Ace**, **Lab**) or tartrate (**Met**) salts. This was achieved using milling.

The general procedure involved weighing out 1.000 g of commercial salt in a 15 mL milling jar together with 1 (**Pro** and **Lab**), 1.5 (**Ace**), or 2 (**Met**) molar equivalents of pre-milled sodium hydroxide pellets. 100 μL of distilled water was then added to the mixture together with two 10 mm ⌀ milling balls. This mixture was milled for a total of 10 minutes at 1500 rpm. For **Pro** and **Met**, the milled material was dissolved in ethyl acetate and the jars washed with water and ethyl acetate. Liquid–liquid extraction was performed, and the ethyl acetate layer dried with anhydrous magnesium sulfate. The solid was filtered off and the remaining solvent removed *in vacuo*. **Ace** and **Lab** were isolated by washing out the milling jars with 25 mL of water. The water was added to a beaker and stirred at room temperature for 1 hour. Thereafter, the free base was filtered off and dried. All the free bases were isolated in high yield (**Pro** = 84%, **Met** = 97%, **Ace** = 81%, **Lab** = 90%).

The crystal structure of the free base of **Ace** is unknown. During our experiments, we isolated single crystals of **Ace** *via* slow evaporation from a methanol solution.

Salification: synthesis and single-crystal growth of salts with beta blockers and NA or INA

The general procedure for preparing the beta blocker salts first involved LAG screening. 80 mg of beta blocker (as the free base) and 1 equivalence of **NA** or **INA** were added to a 5 mL milling jar together with one 7 mm ⌀ milling ball and 30 μL of solvent. Powder X-ray diffraction (PXRD) was performed on the resulting powders to assess the presence of a new phase. When a new phase was evident, single crystals of the salts were then grown by dissolving the crystalline material prepared from LAG in the solvent used for LAG and allowing the solvent to slowly evaporate. The crystals obtained were characterized by single-crystal X-ray diffraction (SCXRD). Thereafter, the simulated PXRD patterns from the obtained single crystal structures were compared to the patterns obtained from the LAG screening. If the experimental patterns showed a mixture of salt and single components, the milling time and number of balls were adjusted. The LAG conditions required to obtain each pure **beta blocker·NA/INA** salt are listed in Table 1.

Salt generation from slow evaporation and seeding

Once single crystals of each **beta blocker·NA/INA** salt were grown and phase-pure salts were obtained from LAG, the likelihood of cocrystallization *via* slow evaporation and seeding was assessed. For both procedures, 50 mg of beta blocker together with 1 equivalence of **NA** or **INA** were dissolved in the solvent used in the successful LAG experiments. For the seeding

Table 1 Summary of LAG conditions used to obtain phase pure **beta blocker·NA/INA** salts

Salt	Solvent	Solvent volume (μL)	η (μL mg^{-1})	Time (min)	No. of balls[a]
Pro·NA	MeCN	30	0.25	3	1
Pro·INA	IPA	30	0.25	3	1
Met·NA	IPA	30	0.26	3	1
Met·INA	MeCN	30	0.26	3	1
Ace·NA	MeCN	30	0.28	20	2
Ace·INA	MeCN	30	0.28	10	2
Ate·NA	MeOH	30	0.26	10	2
Ate·INA	MeCN	30	0.26	10	2
Lab·INA	MeCN	30	0.27	20	2

[a] 7 mm ⌀ milling balls were used in 5 mL jars.

experiments, a spatula tip of the phase pure crystalline material obtained from LAG was added to the solution and then the solvent was allowed to evaporate. Solid material or oils were obtained, and the solids were analyzed *via* PXRD. These results are summarized in Table S5, ESI.†

Effect of liquid additive in milling experiments

Beta blocker·NA/INA salts were obtained *via* LAG with a specific solvent, as shown in Table 1. Thereafter, neat milling and LAG with a series of alternative solvents were tested under the same conditions. In total, 14 LAG experiments (methanol (MeOH), ethanol (EtOH), isopropanol (IPA), ethyl acetate (EtOAc), acetonitrile (MeCN), acetone, tetrahydrofuran (THF), dichloromethane (DCM), chloroform, *N*,*N*-dimethylformamide (DMF), water, diethyl ether (Et_2O), toluene, and hexanes) and a neat milling experiment were performed for each beta blocker salt. The resultant material was analyzed *via* PXRD.

Single crystal X-ray diffraction (SCXRD)

Reflection intensity data were collected at 100 K with the use of an Oxford Cryostream on either a Rigaku XtaLAB Synergy-i Kappa or a Bruker D8 Venture diffractometer. Full details are included in Section 3, ESI.†

Powder X-ray diffraction (PXRD)

PXRD patterns were collected on a Rigaku MiniFlex II or Miniflex 6G benchtop powder diffractometer. The X-ray diffraction pattern was obtained by scanning a 2θ range of 3–60°, step size = 0.02°, and scan time of 5 degree per min. The X-ray source was CuKα radiation ($\lambda = 1.5418$ Å) with an anode voltage of 30 kV and a current of 15 mA (Miniflex II) or 40 kV and 15 mA (Miniflex 6G) with Bragg–Brentano beam geometry. Diffraction intensities were recorded on a D/teX Ultra position sensitive detector. Samples were prepared on zero background holders.

Nuclear magnetic resonance (NMR) spectroscopy

Solution ^{1}H NMR spectra of the phase pure **beta blocker·NA/INA** salts were obtained in DMSO-d_6 on a Bruker Avance III 500 MHz spectrometer. The spectra confirm the 1 : 1 composition of the components in the salts as detailed in Section 6, ESI.†

Thermogravimetric analysis (TGA)

Thermogravimetric analysis was performed on a TA Instruments TGA Q50 operating under a nitrogen atmosphere (40 mL min^{-1}) with a platinum pan. Powdered samples were run at a rate of 10 °C min^{-1}.

Differential scanning calorimetry (DSC)

DSC experiments were performed on a TA Instruments DSC250 equipped with a RCS 90 refrigerated cooling system and under a nitrogen atmosphere (50 mL min^{-1}). Powdered samples were run at a rate of 10 °C min^{-1} in aluminium pans sealed with hermetic lids.

Results and discussion

Mechanochemical neutralization of beta blockers

Besides **Ate**, all four of the other selected beta blockers were commercially purchased as chloride (**Pro**, **Ace**, and **Lab**) or tartrate (**Met**) salts. Although there have been reported cocrystals with salts such as fluoxetine HCl,[40,41] we found that all our attempts to cocrystallize the commercial salts with **NA** or **INA** were unsuccessful. Thus, to facilitate cocrystallization, the salts needed to be neutralized to afford the free base of each beta blocker.

Surprisingly, there are limited reports of using mechanochemistry to neutralize the acid in a pharmaceutical salt, with solution neutralization methods nearly always being employed. This is despite the fact that free bases obtained thereafter are often further subjected to milling in the quest for discovering other multicomponent solids.[42,43] Here, we initially attempted solution neutralizations wherein the commercial beta blocker salt was dissolved in water and a NaOH solution was added dropwise until the solution was neutralized. However, mixtures of the free base and salt were frequently obtained, and without purity checks, this would greatly complicate subsequent cocrystallization experiments.

Exploring other avenues to enable this transformation cleanly, MacGillivray and coworkers recently reported using mechanochemistry to facilitate crystallization of the anhydrous form of the free base opioid, naloxone, from its chloride salt.[44] Taking this as inspiration, we assessed whether the free base of

each beta blocker could be formed in a similar way. On a gram scale, after subjecting the commercial salts to LAG with solid NaOH and 100 μL of water, PXRD of the resultant powders indicated the clear formation of a new phase (the free base). For the commercial HCl salts (**Pro HCl**, **Ace HCl**, and **Lab HCl**), the presence of NaCl was also clearly evident (Fig. S22–S25, ESI†). Upon either extraction or filtration, depending on the beta blocker, the free bases were obtained in excellent yields (81–97%).

Salification of beta blockers

Upon obtaining the pure free bases, LAG experiments with **NA** and **INA** were performed. PXRD demonstrated that new crystalline phases were obtained for 9 of the 10 possibilities, namely, **Pro·NA**, **Pro·INA**, **Met·NA**, **Met·INA**, **Ace·NA**, **Ace·INA**, **Ate·NA**, **Ate·INA**, and **Lab·INA**. Several conditions were used in attempts to prepare a salt of **Lab** with **NA**; however, no conditions afforded salt formation (see Mechanochemical synthesis section and ESI†). Table 1 details the LAG conditions that facilitated pure **beta blocker·NA/INA** salt formation.

Single crystals suitable for SCXRD were grown *via* slow evaporation by dissolving the powders obtained from LAG in the same solvent that was used for LAG. Of the **beta blocker·NA/INA** salts, one of the nine salts had been previously obtained *via* LAG with *n*-butanol and methanol, namely, **Met·NA**.[37] We demonstrate a slightly simpler method utilizing only a single solvent (IPA). The reported **Met·NA** crystal structure (CSD refcode TOPZIK) was collected at 293 K, and here we report the low temperature, 100 K, structure. The other eight salts described here are novel.

Single crystal X-ray structures

All the beta blockers form 1 : 1 salts with **NA** and/or **INA** owing to the large pK_a difference between the components, in accordance with the pK_a rule[21,22] (Table S2, ESI†). All salts formed in centrosymmetric space groups, indicative that all beta blocker stereoisomers crystallized as a mixture. The carboxylic acids of **NA** and **INA** donate their acidic proton to the basic amine on the beta blocker skeleton, resulting in a carboxylate of **NA** or **INA** and the protonated beta blocker (Fig. 2A). The supramolecular synthons responsible for the cocrystallization of the acids with the beta blockers are shown in Fig. 2B. Most of the salts are sustained by synthon 1, which involves a two-point charge-assisted hydrogen bond between the carboxylate and the alkanolamine. Morphologies of hydrogen-bonded arrays are frequently identified using graph-set notation.[45] Synthon 1 is a hydrogen-bonded ring with notation $R_2^2(9)$. Many of the salts also contain synthon 2i, which instead involves a single-point hydrogen bond between the carboxylate and amine. Synthon 2ii involves the carboxylate engaging in hydrogen bonds with protonated amine nitrogen atoms on two beta blocker molecules. Therefore, the beta blocker salts can be categorized into three synthon groupings, which are summarized in Fig. 3.

The chemical structures of **Pro** and **Met** lack additional hydrogen-bond-donor groups outside the alkanolamine skeleton. Thus, most of these salts lack extended hydrogen bonding

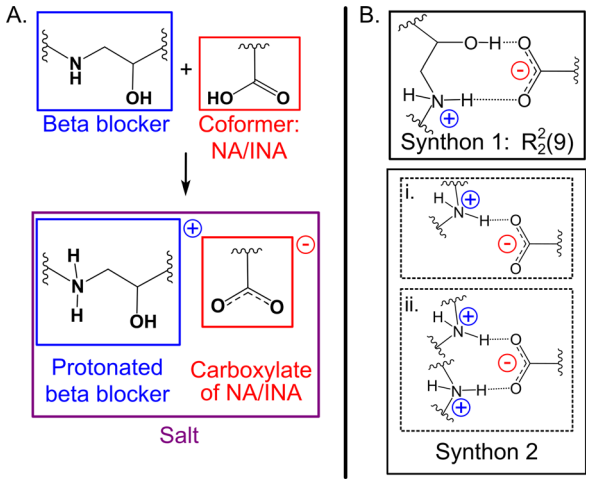

Fig. 2 (A) Salt formation illustrating donation of the acidic proton of NA or INA to the basic amine on the beta blocker alkanolamine skeleton. (B) The two charge-assisted hydrogen bond synthons observed in the **beta blocker·NA/INA** salts. Synthon 2 was observed in two variations; the carboxylate either interacts with one distinct protonated amine (i), which is present together with synthon 1, or the carboxylate interacts with two distinct protonated amines (ii).

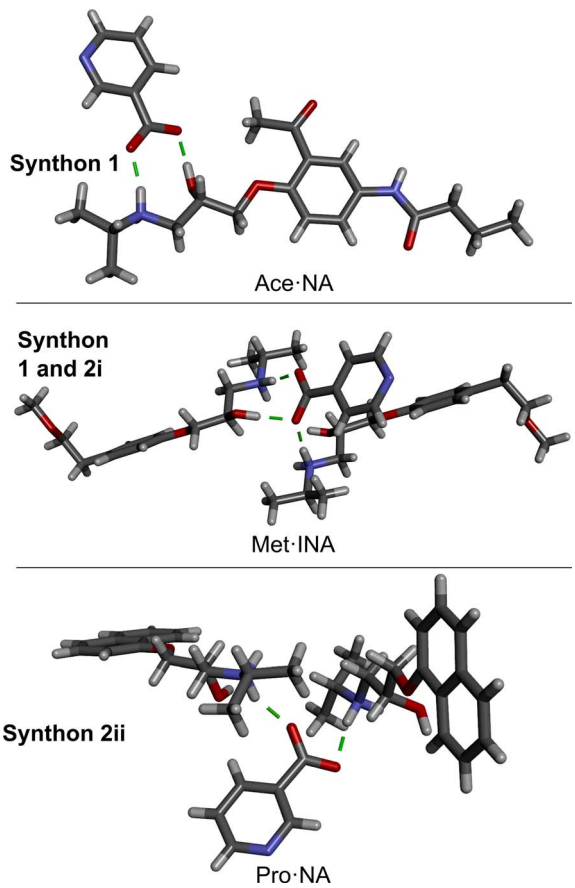

Fig. 3 Molecular structures as determined by SCXRD, illustrating the three synthon groupings present in the **beta blocker·NA/INA** salts. A representative structure for each category is shown. Hydrogen bonds are shown with green lines.

Table 2 Relevant parameters from X-ray crystal structures of **beta blocker·NA/INA** salts. The synthons are shown in Fig. 2B, and the distances are related to those synthons

Salt	Space group	Primary synthon(s)	$d_{O\cdots N}$[a] (Å)	$d_{O\cdots O}$ (Å)
Pro·NA	$P2_1/c$	2ii	2.767(2)	
			2.850(2)	
Pro·INA	$P\bar{1}$	1 and 2i	2.793(2)	2.681(1)
			2.758(2)	
Met·NA	$P\bar{1}$	1 and 2i	2.751(1)	2.707(1)
			2.797(1)	
Met·INA	$P\bar{1}$	1 and 2i	2.762(1)	2.695(1)
			2.789(1)	
Ace·NA[b]	$P\bar{1}$	1	2.692(2)	2.513(1)
			2.694(2)	2.494(1)
			2.685(2)	2.504(1)
Ace·INA[b]	$P\bar{1}$	1	2.695(4)	2.502(3)
			2.731(4)	2.486(3)
			2.709(4)	2.507(3)
Ate·NA	$P\bar{1}$	1 and 2i	2.763(2)	2.679(2)
			2.783(2)	
Ate·INA	$P2_1/c$	1 and 2i	2.774(1)	2.709(1)
			2.822(1)	
Lab·INA	$P\bar{1}$	2ii	2.740(2)	
			2.854(2)	

[a] For solids containing synthon 1 and 2i, the first distance is for synthon 1 and the second is for synthon 2i. [b] There are three pairs of molecules (six molecules total) in the asymmetric unit. All other salts contained one set of molecules in their respective asymmetric units.

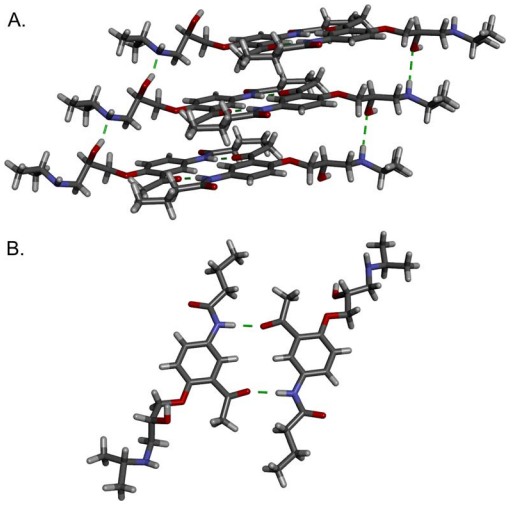

Fig. 4 Single crystal structure of **Ace** highlighting (A) hydrogen-bonded chains involving alkanolamine and (B) hydrogen-bonded dimer with amide and ketone groups. Disorder in the alkanolamine chain is omitted for clarity; thus, only the *R* stereoisomer is depicted.

in the solid state. On the other hand, **Ace**, **Ate**, and **Lab** all contain an amide functional group, which facilitates formation of extended hydrogen-bonded sheets/networks. Notably, solvates were formed for the **Ate** salts, namely, **Ate·NA** with MeOH and **Ate·INA** with MeCN. No solvates were observed with any of the other beta blocker salts. In many of the salts, the pyridine groups of **NA** or **INA** interact through weaker N···H–C hydrogen bonding. Some structural details are in Table 2, and full crystal packing descriptions with additional figures are provided in the ESI, Section 4.2.†

Conventional, solution-based cocrystallization experiments using either slow evaporation (without LAG beforehand) or seeding (using powder obtained from LAG) were reasonably successful when the same solvent used in LAG was employed, but not in all cases (Table S5, ESI†).

During our experiments, we also successfully isolated single crystals of the free base of **Ace**, for which the structure has not been reported. **Ace** crystallized in the space group $P\bar{1}$ with one unique molecule in the asymmetric unit. Both enantiomers are present in the structure through disorder of the alkanolamine chain. The alkanolamine groups engage in hydrogen bonds to form infinite 1D chains (Fig. 4a). The chains are connected through hydrogen-bonded dimers that form between the ketone and amide of two **Ace** molecules (Fig. 4b). Full details are provided in the ESI.†

Mechanochemical salification

The optimized conditions that afford successful salt formation *via* mechanochemistry can be grouped into three categories. The **Pro** and **Met** salts contain beta blockers with similar chemical structures that lack additional hydrogen-bond donors (outside the alkanolamine) and require short milling times (three min) with one milling ball to achieve full conversion. The second grouping is of **Ace·INA** and both **Ate** salts. The beta blockers involved here both contain an amide group in addition to the alkanolamine, and a milling time of 10 min with two milling balls was required to achieve full conversion to the salts. The last category consists of **Ace·NA** and **Lab·INA**. **Lab** contains an amide and phenol in addition to the alkanolamine, and the compound has two stereocenters (mixture of all four stereoisomers). These two salts required a milling time of 20 min and two milling balls to afford full salt conversion.

Bučar, Hasa, and coworkers have demonstrated the impact of liquid additives on cocrystallization *via* LAG.[29] Specifically, the team showed liquid additives could be divided into three classes: catalytic, inhibitive, and prohibitive. Liquids classified as catalytic enabled salt formation, inhibitive slowed salt formation, and prohibitive precluded salt formation. While liquids within these categories will differ for each system, the study showed the importance of screening more than one liquid additive before assessing mechanochemical outcomes.

To investigate the influence of liquid additives on the mechanochemical preparation of the nine beta blocker salts, the efficiency of salt formation was assessed across a selection of solvents. Specifically, neat milling (*i.e.*, absence of solvent) and LAG with a total of 14 different liquid additives was conducted. The liquid additives represent a range of polarities (water through hexanes ordered in Fig. 5 and Fig. 6 according to the polarity empirical parameter reported by Reichardt and Welton,[46] see Table S7, ESI†) and the polar solvents include both protic and aprotic solvents. The optimized conditions that afforded successful salt formation (Table 1) were used for each experiment, and the liquid additive was the only variable changed. Thus, the subsequent discussion regarding conversion is relative to the optimized conditions for each respective

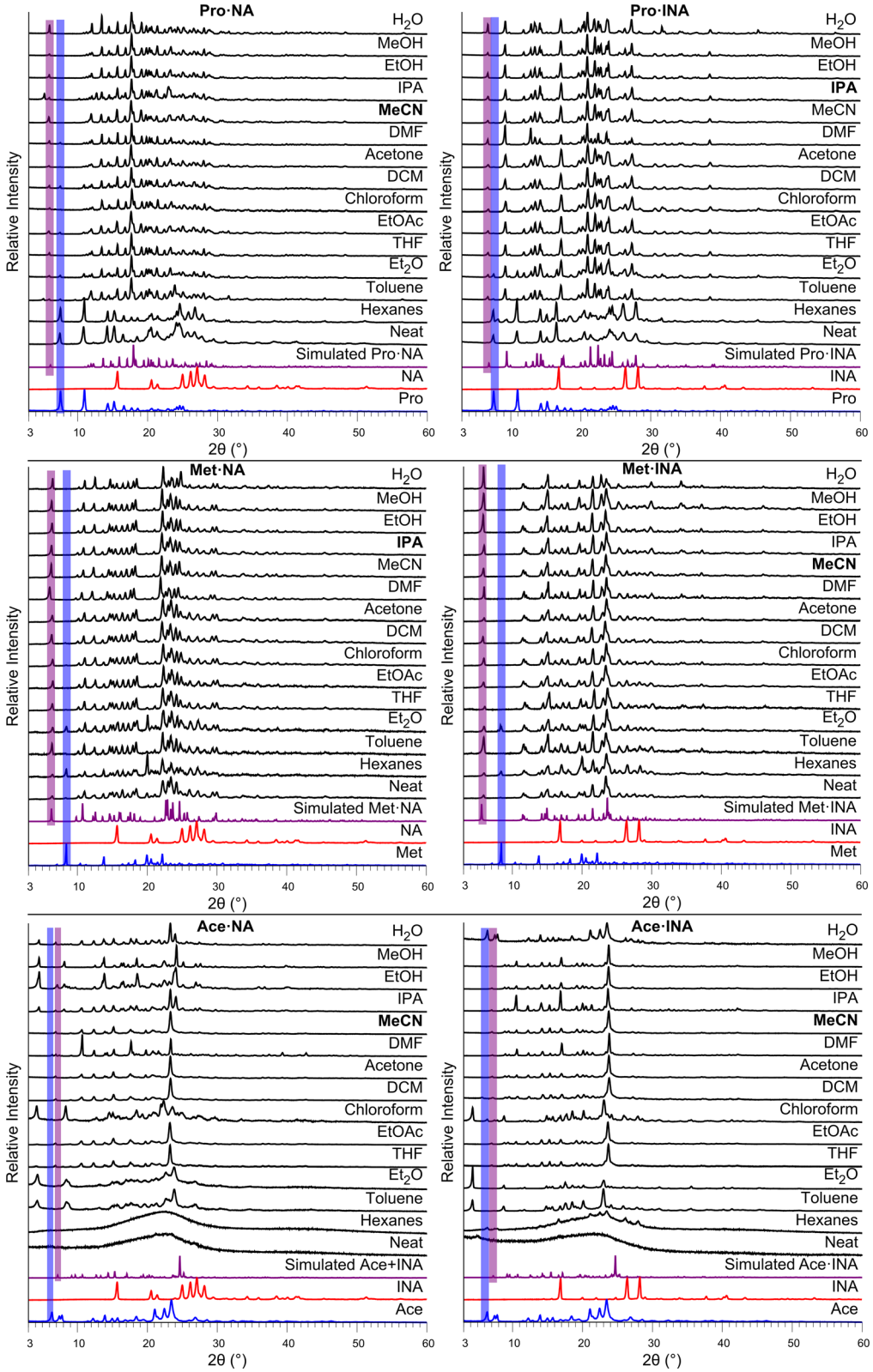

Fig. 5 PXRD patterns illustrating the effect of solvent polarity on the outcome of the mechanochemical synthesis of the **Pro**, **Met**, and **Ace** salts. Solvents are ordered from the most polar (top) to the least with the solvent used to grow single crystals of the salt in bold. The purple (salt) and blue (free base beta blocker) highlighted peaks indicate the characteristic reference peaks used to determine each patterns' composition (pure salt, mixture of salt and components, components only, and presence of unknown phase(s)).

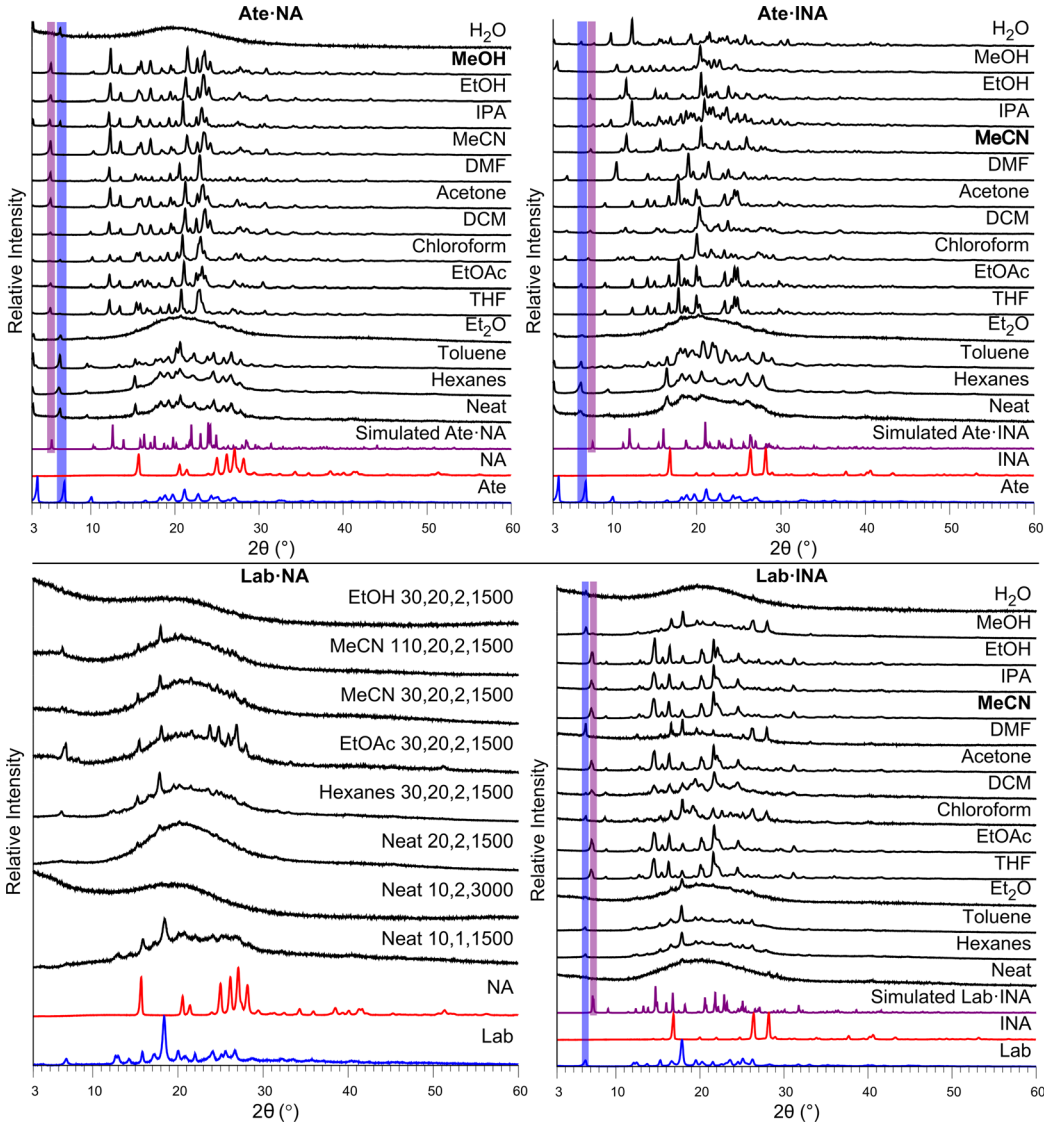

Fig. 6 PXRD patterns illustrating the effect of solvent polarity on the outcome of the mechanochemical synthesis of the **Ate** and **Lab** salts. Solvents are ordered from the most polar (top) to the least with the solvent used to grow single crystals of the salt in bold. The purple (salt) and blue (free base beta blocker) highlighted peaks indicate the characteristic reference peaks used to determine each patterns' composition (pure salt, mixture of salt and components, components only, and presence of unknown phase(s)). For **Lab·NA**, a new crystalline phase was not identified, and single crystals were not grown. The displayed patterns illustrate various conditions attempted resulting in the components and/or amorphous phases present. For the LAG experiments, the numbers following the solvent label indicate mechanochemistry conditions of the solvent amount (μL), time (minutes), number of 7 mm ⌀ balls, and speed (rpm). The neat milling conditions omit the solvent amount.

salt. PXRD was used to assess the solid phases. For each system, the free base of the beta blocker and the **beta blocker·NA/INA** salt exhibit unique signals in their PXRD patterns below 10° 2θ; thus, identification of the salt, individual components, other unknown phases, or mixtures could be accomplished. A summary of the milling results is shown in Table 3, and larger versions of each plot in Fig. 5 and 6 can be found in the ESI, Fig. S26–S35.†

Neat milling was generally unsuccessful. Partial formation of salts occurred only with **Met**. Thus, LAG is broadly more useful for this class of beta blockers.

In the case of **Pro**, salt formation occurred with all solvents except in the case of hexanes for **Pro·NA** (Fig. 5, top). The lowest polarity solvents resulted in incomplete conversion to the salts. Complete conversion for both **Pro·NA** and **Pro·INA** occurred with THF, chloroform, as well as the three highest polarity and protic solvents, EtOH, MeOH, and H_2O. Broader solvent success was seen for **Pro·INA** as DCM, DMF, and IPA also afforded full conversion.

Met salt formation with **NA** or **INA** occurs for all solvents, irrespective of polarity (Fig. 5, middle). However, the degree of formation differs across polarity with the least polar solvents resulting in a mixture of salt and components. Interestingly, for **Met·INA**, toluene displays complete salt formation, being the only exception. The solvents, beginning with acetone and

Table 3 Summary highlighting the degree of conversion achieved using liquid additives of different polarities in the formation of the **beta blocker·NA/INA** salts

	Least polar														Most polar
Salt	Neat	Hexanes	Toluene	Et_2O	THF	EtOAc	Chloroform	DCM	Acetone	DMF	MeCN	IPA	EtOH	MeOH	H_2O
Pro·NA	x	x	~	~	√	~	√	~	~	~	√	~	√	√	√
Pro·INA	x	~	~	~	√	~	√	√	~	√	~	√	√	√	√
Met·NA	~	~	~	~	~	√	~	~	√	√	√	√	√	√	√
Met·INA	~	~	√	~	√	~	~	√	√	√	√	√	√	√	√
Ace·NA	x	x	*	*	~	~	*	√	√	~	√	~	*	*	~
Ace·INA	x	x	*	*	√	√	*	~	√	√	√	√	√	√	x
Ate·NA	x	x	x	x	~	√	~	√	~	~	√	~	~	√	x
Ate·INA	x	x	~	x	*	*	~	~	*	*	√	~	~	*	~
Lab·INA	x	x	x	x	√	√	*	~	√	x	√	√	√	~	x

Key	
√	Complete salt conversion. Thick box outline illustrates solvent from which single crystals were grown
~	Incomplete conversion where components and/or unknown phases(s) are present
x	No salt formation with only components present
*	Unknown phase(s) with or without components

encompassing all solvents of higher polarity (aprotic or protic), afforded complete conversion to the **Met** salts.

The results for the **Ace** salts do not illustrate a clear polarity trend (Fig. 5, bottom) with several solvents indicating the presence of an unknown phase(s) (toluene, Et_2O, and chloroform for both salts and, additionally, EtOH and MeOH for **Ace·NA**). Full conversion to the salt was observed for DCM, acetone, and MeCN for **Ace·NA** while full conversion was afforded with THF, EtOAc, acetone, DMF, MeCN, IPA, EtOH, and MeOH with **Ace·INA**. Interestingly, water demonstrated partial conversion for **Ace·NA** but no formation of **Ace·INA**.

Ate, being the only beta blocker which formed solvated salts, showed significant variability with different solvents (Fig. 6, top). For **Ate·NA**, the least polar solvents, namely hexanes, toluene and Et_2O showed no salt formation while solvents of higher polarity facilitated salt formation differing by the extent of conversion. EtOAc, DCM, MeCN, and MeOH afforded complete conversion. Notably, H_2O showed no formation of the salt. **Ate·INA** exhibited similar behavior, with the exception of toluene and H_2O showing partial salt formation. Furthermore, several solvents show the appearance of an unknown phase(s) (THF, EtOAc, acetone, DMF, MeOH) with only MeCN showing complete salt formation. Given the formation of salt-solvates with **Ate**, the additional phases may be solvatomorphs (although we were unable to grow single crystals).

In the case of **Lab**, salt formation with **INA** occurs with THF, EtOAc, DCM, acetone, MeCN, IPA, EtOH, and MeOH. All low polarity solvents fail to afford salt formation (Fig. 6, bottom). Full conversion to the salt was observed with all the solvents mentioned above except DCM and MeOH.

When mechanochemistry was used to prepare a salt with **Lab** and **NA**, no conditions were found to afford a new crystalline phase (Fig. 6, bottom). The solvent volume, milling time, number of milling balls, and milling speed (rpm) were varied. Given the broad success with EtOAc, MeCN, and EtOH in yielding salt formation with the other beta blockers (including **Lab·INA**), variations to the conditions with these solvents were the focus. Neat milling and a nonpolar solvent additive (hexanes) were also tried. However, all experiments yielded amorphous material or single components. Some representative experimental results are shown in Fig. 6. Considering that **Lab** is a mixture of four stereoisomers, it may not be surprising that a crystalline phase was not found. As previously mentioned, there is only one published single-crystal X-ray structure of **Lab**, the hydrochloride salt. Here, we isolated the first multicomponent solid of **Lab** containing a coformer, namely, **Lab·INA**, and multiple solvents afford the pure salt. The subtle difference in the position of the nitrogen on the pyridine ring of **NA** and **INA** clearly plays a larger than anticipated role in facilitating cocrystallization of **Lab**.

For the beta blocker APIs, broadly, more polar liquid additives aided in successful salt formation, although the extent of conversion differed considerably (Table 3). It is clear that the polarity of the solvent is not the only possible parameter to use in evaluating salt formation, especially when considering the extent of conversion. We also examined solvent properties including the Hildebrand solubility parameter, dielectric constant, and dipole moment,[46,47] but a clearer correlation to salt conversion was not apparent (Tables S7–S10, ESI†).

Revisiting the work of Bučar, Hasa, and coworkers,[29] the liquid additives used here do not fall into clear categories as

there are substantial variations between beta blockers and even between the two salts of individual beta blockers themselves. Bučar, Hasa, and coworkers clearly demonstrate that using any liquid additive in a mechanochemical screening or synthesis process does not always enhance cocrystallization and further suggest that screening multiple solvents be an important aspect of crystal form development. In line with this prior work, the results described here further demonstrate the utility of different liquid additives in attaining complete, partial, or no conversion to multicomponent solids of beta blockers and the role of liquid additives in mechanochemical reactions is far from trivial. Moreover, use of different liquid additives allows exploration into the multicomponent crystal landscape,[48] especially considering the appearances of multiple and/or unidentified phases (here, in the case of the two **Ace** salts, **Ate·INA**, and **Lab·INA**). As **Ace** and **Ate** are racemic mixtures and **Lab** is an equal mixture of all four stereoisomers, these additional phases may be a result of spontaneous resolution of stereoisomers and the formation of conglomerates. Other solvates, salt polymorphs, or individual component polymorphs are also possible. Unfortunately, we were unable to obtain single crystals of additional unknown forms.

Thermal properties following salification

We also investigated the thermal stability of the **beta blocker·NA/INA** salts, and Fig. 7 illustrates the DSC traces of the commercial beta blocker salts, their respective free bases, and the **NA/INA** salts. In the case of **Pro**, **Met**, and **Ace**, salification increases the melting point compared to the free bases. This is particularly notable for **Met**, where its low melting point (~53 °C) more than doubles upon salt formation and the values are similar to the commercial tartrate form. **Ate** and **Lab** possess lower melting points upon salt formation. In the case of **Ate**, this could be due to the presence of solvent in the solid, which was further confirmed through TGA. TGA of each **beta blocker·NA/INA** salt demonstrated similar decomposition onset temperatures when compared to the free bases (Fig. S45–S49, ESI†).

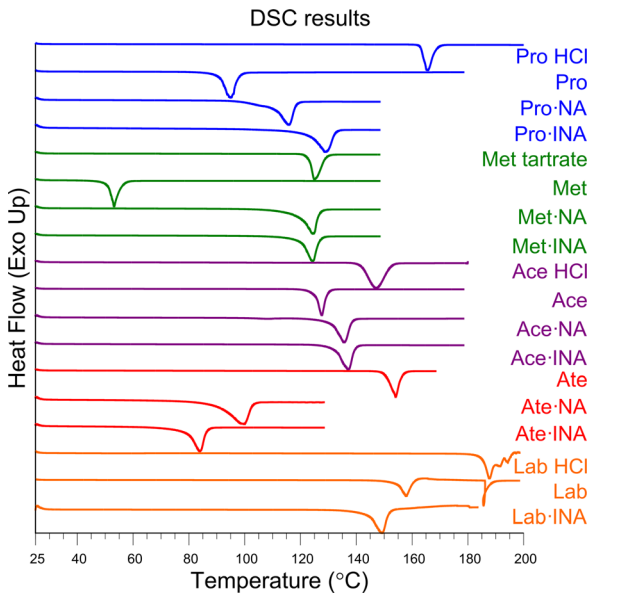

Fig. 7 DSC results of the commercial beta blocker salts, free bases, and beta blocker·NA/INA salts illustrating their melting points.

Conclusions

In conclusion, we have described the use of mechanochemistry in effectively facilitating the salification of five beta blockers (**Pro**, **Met**, **Ace**, **Ate**, and **Lab**) with **NA** and **INA**. Commercial beta blocker salts were handily neutralized *via* mechanochemistry on a gram scale. Thereafter, protonation of the basic amine on the alkanolamine of the beta blocker free bases was found to be key to salt formation with charge-assisted hydrogen bonding facilitating cocrystallization. With approximately 20 beta blockers on the market, we expect this study to be applicable to other beta blockers where salification can be used to improve the properties of any API in this class at large. In the LAG studies, the effect of different liquid additives on the salification process showed that the solvent used plays a substantial role in the milling outcome and does not simply correlate to polarity for this selection of compounds. These results illustrate the utility of screening with a multitude of different liquid additives, which is analogous to solvent screening in organic synthesis and solution crystallization. Implementing solvent screening experiments in LAG will likely assist in exploring more of the crystal landscape and thereby aid in the efficient discovery of additional crystal forms during solid form development and/or de-risk late-stage polymorph appearances.

Data availability

The data supporting this article have been included as part of the ESI. Crystallographic data for **Pro·NA**, **Pro·INA**, **Met·NA**, **Met·INA**, **Ace**, **Ace·NA**, **Ace·INA**, **Ate·NA**, **Ate·INA**, and **Lab·INA** have been deposited at the Cambridge Crystallographic Data Centre under 2371670–2371679.†

Author contributions

D. S. B. carried out investigation, validation, formal analysis, data curation, visualization, and writing and editing of the original draft. J. D. L. carried out conceptualization, investigation, formal analysis, and data curation. M. G., B. B. N., and M. I. A. contributed to the investigation and G. C. G. III and D. K. U. undertook formal analysis and data curation. K. M. H. was responsible for conceptualization, funding acquisition, project administration, supervision, and writing, reviewing, and editing of the original draft. All authors read and approved the final manuscript.

Conflicts of interest

There are no conflicts to declare.

Acknowledgements

This work was supported in part by The Welch Foundation (D-2068-20210327 to K. M. H.). B. B. N. acknowledges financial support from the Texas Tech University Honors College Undergraduate Research Scholars program. M. I. A. acknowledges financial support from the Texas Tech University College to Career Program. The work was also supported in part by the University of Missouri (including an instrument grant CHE-89-08304). The authors thank Dr Steven Kelley for helpful crystallographic discussions.

References

1 D. Braga, L. Maini and F. Grepioni, *Chem. Soc. Rev.*, 2013, **42**, 7638–7648.
2 M. C. Etter, S. M. Reutzel and C. G. Choo, *J. Am. Chem. Soc.*, 1993, **115**, 4411–4412.
3 M. R. Caira, L. R. Nassimbeni and A. F. Wildervanck, *J. Chem. Soc., Perkin Trans. 2*, 1995, 2213–2216.
4 S. L. James, C. J. Adams, C. Bolm, D. Braga, P. Collier, T. Friscic, F. Grepioni, K. D. Harris, G. Hyett, W. Jones, A. Krebs, J. Mack, L. Maini, A. G. Orpen, I. P. Parkin, W. C. Shearouse, J. W. Steed and D. C. Waddell, *Chem. Soc. Rev.*, 2012, **41**, 413–447.
5 S. Aitipamula, R. Banerjee, A. K. Bansal, K. Biradha, M. L. Cheney, A. R. Choudhury, G. R. Desiraju, A. G. Dikundwar, R. Dubey, N. Duggirala, P. P. Ghogale, S. Ghosh, P. K. Goswami, N. R. Goud, R. R. K. R. Jetti, P. Karpinski, P. Kaushik, D. Kumar, V. Kumar, B. Moulton, A. Mukherjee, G. Mukherjee, A. S. Myerson, V. Puri, A. Ramanan, T. Rajamannar, C. M. Reddy, N. Rodriguez-Hornedo, R. D. Rogers, T. N. G. Row, P. Sanphui, N. Shan, G. Shete, A. Singh, C. C. Sun, J. A. Swift, R. Thaimattam, T. S. Thakur, R. Kumar Thaper, S. P. Thomas, S. Tothadi, V. R. Vangala, N. Variankaval, P. Vishweshwar, D. R. Weyna and M. J. Zaworotko, *Cryst. Growth Des.*, 2012, **12**, 2147–2152.
6 S. S. Bharate, *Drug Discovery Today*, 2021, **26**, 384–398.
7 G. Bolla, B. Sarma and A. K. Nangia, *Chem. Rev.*, 2022, **122**, 11514–11603.
8 A. J. Smith, P. Kavuru, L. Wojtas, M. J. Zaworotko and R. D. Shytle, *Mol. Pharm.*, 2011, **8**, 1867–1876.
9 D. Li, J. Li, Z. Deng and H. Zhang, *CrystEngComm*, 2019, **21**, 4145–4149.
10 J. Wang, X.-L. Dai, T.-B. Lu and J.-M. Chen, *Cryst. Growth Des.*, 2021, **21**, 838–846.
11 M. K. Bommaka, M. K. C. Mannava, K. Suresh, A. Gunnam and A. Nangia, *Cryst. Growth Des.*, 2018, **18**, 6061–6069.
12 B. Saikia, P. Bora, R. Khatioda and B. Sarma, *Cryst. Growth Des.*, 2015, **15**, 5593–5603.
13 G. L. Amidon, H. Lennernäs, V. P. Shah and J. R. Crison, *Pharm. Res.*, 1995, **12**, 413–420.
14 J. M. Ting, W. W. Porter III, J. M. Mecca, F. S. Bates and T. M. Reineke, *Bioconjugate Chem.*, 2018, **29**, 939–952.
15 R. Thipparaboina, D. Kumar, R. B. Chavan and N. R. Shastri, *Drug Discovery Today*, 2016, **21**, 481–490.
16 N. K. Duggirala, M. L. Perry, O. Almarsson and M. J. Zaworotko, *Chem. Commun.*, 2016, **52**, 640–655.
17 C. Almansa, R. Mercè, N. Tesson, J. Farran, J. Tomàs and C. R. Plata-Salamán, *Cryst. Growth Des.*, 2017, **17**, 1884–1892.
18 O. N. Kavanagh, D. M. Croker, G. M. Walker and M. J. Zaworotko, *Drug Discovery Today*, 2019, **24**, 796–804.
19 G. R. Desiraju, *Angew. Chem.*, 2003, **34**, 2311–2327.
20 U.S. Food and Drug Administration, *Substances Added to Food (formerly EAFUS)*, **https://www.cfsanappsexternal.fda.gov/scripts/fdcc/?set=FoodSubstances**, accessed 27 February 2024.
21 S. L. Childs, G. P. Stahly and A. Park, *Mol. Pharm.*, 2007, **4**, 323–338.
22 A. J. Cruz-Cabeza, *CrystEngComm*, 2012, **14**, 6362–6365.
23 D. Douroumis, S. A. Ross and A. Nokhodchi, *Adv. Drug Delivery Rev.*, 2017, **117**, 178–195.
24 Y. Xiao, C. Wu, X. Hu, K. Chen, L. Qi, P. Cui, L. Zhou and Q. Yin, *Cryst. Growth Des.*, 2023, **23**, 4680–4700.
25 J.-L. Do and T. Friščić, *ACS Cent. Sci.*, 2017, **3**, 13–19.
26 J. D. Loya, S. J. Li, D. K. Unruh and K. M. Hutchins, *Cryst. Growth Des.*, 2022, **22**, 285–292.
27 L. Ma, Q. Zheng, D. K. Unruh and K. M. Hutchins, *Chem. Commun.*, 2023, **59**, 7779–7782.
28 T. Friščić, S. L. Childs, S. A. A. Rizvi and W. Jones, *CrystEngComm*, 2009, **11**, 418–426.
29 M. Arhangelskis, D. K. Bučar, S. Bordignon, M. R. Chierotti, S. A. Stratford, D. Voinovich, W. Jones and D. Hasa, *Chem. Sci.*, 2021, **12**, 3264–3269.
30 P. Sacchi, S. E. Wright, P. Neoptolemou, G. I. Lampronti, A. K. Rajagopalan, W. Kras, C. L. Evans, P. Hodgkinson and A. J. Cruz-Cabeza, *Proc. Natl. Acad. Sci. U.S.A.*, 2024, **121**, e2319127121.
31 E. Oliver, F. Mayor Jr and P. D'Ocon, *Rev. Española Cardiol.*, 2019, **72**, 853–862.
32 A. Martinez, M. Lakkimsetti, S. Maharjan, M. A. Aslam, A. Basnyat, S. Kafley, S. S. Reddy, S. S. Ahmed, W. Razzaq, S. Adusumilli and U. A. Khawaja, *Cureus*, 2023, **15**, e44043.
33 Y. Yang, P. J. Faustino, D. A. Volpe, C. D. Ellison, R. C. Lyon and L. X. Yu, *Mol. Pharm.*, 2007, **4**, 608–614.
34 Y. Tsume and G. L. Amidon, *Mol. Pharm.*, 2010, **7**, 1235–1243.
35 L. Poirier and S. W. Tobe, *Can. J. Cardiol.*, 2014, **30**, S9–S15.
36 P. Murray-Rust, J. Murray-Rust, D. Hartley, P. Hallett and J. Clifton, *Acta Crystallogr., Sect. C: Cryst. Struct. Commun.*, 1984, **40**, 825–828.
37 M. A. Ciciliati, M. E. S. Eusébio, M. R. Silva, É. T. G. Cavalheiro and R. A. E. Castro, *CrystEngComm*, 2019, **21**, 4319–4328.
38 P. L. Canner, K. G. Berge, N. K. Wenger, J. Stamler, L. Friedman, R. J. Prineas and W. Friedewald, *J. Am. Coll. Cardiol.*, 1986, **8**, 1245–1255.
39 L. A. Carlson, *J. Intern. Med.*, 2005, **258**, 94–114.
40 S. L. Childs, L. J. Chyall, J. T. Dunlap, V. N. Smolenskaya, B. C. Stahly and G. P. Stahly, *J. Am. Chem. Soc.*, 2004, **126**, 13335–13342.
41 A. A. Peach, S. T. Holmes, L. R. MacGillivray and R. W. Schurko, *CrystEngComm*, 2023, **25**, 213–224.

42 W. Xing, C. Xing, M. Liu, H. Yu, B. Zhang, S. Yang, N. Gong, Y. Lu and G. Du, *J. Mol. Struct.*, 2023, **1291**, 136029.
43 S. K. Rai, A. Gunnam, M. K. C. Mannava and A. K. Nangia, *Cryst. Growth Des.*, 2020, **20**, 1035–1046.
44 C. Ortiz-de Leon, C. J. Hartwick, C. A. Stuedemann, N. K. Brogden and L. R. MacGillivray, *Cryst. Growth Des.*, 2022, **22**, 6622–6626.
45 M. C. Etter, *Acc. Chem. Res.*, 1990, **23**, 120–126.
46 C. Reichardt and T. Welton, in *Solvents and Solvent Effects in Organic Chemistry*, 2010, pp. 549–586, DOI: **10.1002/9783527632220.app1**.
47 A. F. M. Barton, *CRC Handbook of Solubility Parameters and Other Cohesion Parameters*, CRC Press, 1991.
48 G. R. Desiraju, *Acta Crystallogr., Sect. B: Struct. Sci., Cryst. Eng. Mater.*, 2017, **73**, 775–778.